

# AN APPLICATION OF PSEUDO-SPECTRAL DISCRETIZATION IN MODELLING OF UNSYMMETRICAL TRANSMISSION LINES

Rastko Živanović  
The University of Adelaide, Australia  
rastko@eleceng.adelaide.edu.au

Roberto Schulze and Peter Schegner  
Technical University Dresden, Germany  
roberto.schulze@tu-dresden.de and  
schegner@ieeh.et.tu-dresden.de

**Abstract** – This paper explains how to convert a distributed-parameter model of an unsymmetrical transmission line for specific boundary conditions into a system of Ordinary Differential Equations (ODEs). This approach can be used to study switching transients on transmission lines or to develop new algorithms for line parameter identification. The main technique in the process of model conversion is spatial discretization achieved by using the Chebyshev pseudo-spectral method. The key quality of this approach lies in the application of the Lagrange polynomial interpolation with barycentric weights to represent change of a variable in space and to formulate operators for spatial derivatives. Approximation accuracy for a specific spatial grid resolution can be determined by evaluating coefficients of the Chebyshev polynomial expansion. These are computed from the Lagrange interpolation using Discrete Cosine Transform (DCT). The numerical example is presented to demonstrate application of the method in simulating distributed-parameter unsymmetrical lines during switching events.

**Keywords:** transmission line model, pseudo-spectral discretization, interpolation

## 1 INTRODUCTION

The method for parameter identification of unsymmetrical transmission lines, based on fault records, has been presented recently [1]. The method requires synchronously sampled fault data at both line terminals and it relies on the lumped parameter line model which is general enough to represent unsymmetrical lines. This approach has been further improved by using the advanced Prony method [2] for modeling and filtering of recorded voltage and current signals, preceding the parameter identification stage [3]. In this paper we propose a novel distributed parameter model, based on the Chebyshev pseudo-spectral discretization in space [4], to represent unsymmetrical transmission lines. It is expected that such model will further improve the parameter identification method.

In general transmission line model consists of frequency-dependent parameters [5] (e.g. to model change of resistance due to skin effect), and in some cases time-dependent parameters [6] (e.g. line capacitance variation can be due to corona which depends on instantaneous voltage value). Also spatial variation in parameter values is possible, e.g. due to uneven line height. In order to describe events that are exciting high frequencies on

complex line structures these detailed models are necessary. The novel computational method proposed in this paper assumes frequency independent and spatially uniform parameters. Unsymmetrical transmission line is modeled using constant distributed parameters [7], i.e. using a system of Partial Differential Equations (PDEs) with constant coefficients. Application of the Chebyshev pseudo-spectral discretization to more detailed models will be discussed in the future paper.

The remainder of this paper is organized as follows: the Chebyshev pseudo-spectral discretization in space of the unsymmetrical transmission line PDEs is presented in Section 2; then in Section 3 we explain, using an example, how to include boundary conditions, and how to formulate and solve the resulting system of Ordinary Differential Equations (ODEs); and in the final subsection of Section 3 we present simulation results and discuss some numerical properties of the method.

## 2 SPACE DISCRETIZATION OF TRANSMISSION LINE MODEL

The system of Partial Differential Equations (PDEs) representing unsymmetrical transmission line with constant parameters is:

$$\mathbf{A} \frac{\partial}{\partial t} \mathbf{y}(x, t) = \mathbf{B} \mathbf{y}(x, t) + \frac{\partial}{\partial x} \mathbf{y}(x, t), \quad (1)$$

where

$$\mathbf{y}(x, t) = [\mathbf{v}(x, t)^T \quad \mathbf{i}(x, t)^T]^T, \quad \mathbf{y}(x, t) \in \mathbf{R}^{N_y},$$

and

$$\mathbf{A} = -\begin{bmatrix} \mathbf{0} & \mathbf{L} \\ \mathbf{C} & \mathbf{0} \end{bmatrix}, \quad \mathbf{B} = \begin{bmatrix} \mathbf{0} & \mathbf{R} \\ \mathbf{G} & \mathbf{0} \end{bmatrix}.$$

$\mathbf{v}(x, t)$ ,  $\mathbf{i}(x, t)$  are vectors containing voltages and currents respectively in each phase at time  $t$  and position  $x$  along the line. The matrices  $\mathbf{L}$ ,  $\mathbf{C}$ ,  $\mathbf{R}$  and  $\mathbf{G}$  contain unsymmetrical per-unit-length line parameters.

### 2.1 Chebyshev interpolation

The transmission line model (1) is converted into a system of ODEs through the method of space discretization. First, the space variable  $x$  is projected from the physical domain  $[0, l]$ , where  $l$  is a line length, to the

computational domain  $[-1,1]$  via the following mapping:  $(2/l)x-1 \rightarrow x$ . Second, all of the variables in the model (1),  $y_k(x,t)$ ,  $k=1,2,\dots,N_y$  (included in the vector  $\mathbf{y}(x,t)$ ) are approximated using the Lagrange polynomial interpolation [8]:

$$y_k(x,t) = \sum_{j=0}^N y_k(x_j,t) \phi_j(x), \quad (2)$$

$$\text{where } \phi_j(x) = \frac{c_j}{x-x_j} \bigg/ \sum_{p=0}^N \frac{c_p}{x-x_p} \quad (3)$$

is the barycentric representation of the Lagrange polynomial corresponding to the node  $x_j$  with the weights defined as

$$c_j = \begin{cases} (-1)^j/2 & \text{for } j=0 \text{ or } j=N, \\ (-1)^j & \text{otherwise.} \end{cases}$$

The interpolant (2), i.e. lookup table:  $(x_j, y_k(x_j,t))$ , is defined on the grid of  $N+1$  points

$$x_j = -\cos(j\pi/N), \quad j=0,1,\dots,N,$$

which are the extreme points of the Chebyshev polynomial in the interval  $[-1, 1]$  and including the boundary points [8]. These points are unevenly spaced with higher density on the edges of the interval. They can be visualized in Fig. 1 as the projections on the  $[-1, 1]$  interval ( $x$  - axis) of equispaced points on the upper half of the unit circle ( $\theta$  - axis). In addition, Fig. 1 shows how cosine waves in the  $\theta$  - plane correspond to the Chebyshev polynomials on a non-uniform grid in the  $xy$  - plane. Hence, the Discrete Cosine Transform (DCT) can be used to convert the interpolants (2) into the following approximation based on a linear combination of Chebyshev polynomials [9]:

$$y_k(\theta,t) = \sum_{j=0}^N a_j(t) \cos(j\theta), \quad (4)$$

in the  $\theta$  - plane, which is in the  $xy$  - plane,

$$y_k(x,t) = \sum_{j=0}^N a_j(t) T_j(x), \quad (5)$$

where

$$T_0(x)=1, \quad T_1(x)=x, \quad T_{j+1}(x)=2xT_j(x)-T_{j-1}(x),$$

and  $a_j(t)$  are time-varying coefficients of the expansion.

## 2.2 Differentiation matrix

Approximations of the spatial derivatives of the variables  $\mathbf{y}(x,t)$  are required to perform spatial discretization of the system of PDEs (1) representing line model. These approximations are global and derived by differentiating the interpolation formula (2) with respect to  $x$ :

$$y'_k(x_i,t) = \sum_{j=0}^N (\mathbf{D}_N)_{ij} y_k(x_j,t),$$

$$i=0,1,\dots,N, \quad k=1,2,\dots,N_y \quad (6)$$

where

$$(\mathbf{D}_N)_{ij} = (2/l) \phi'_j(x_i) = (2/l) \frac{c_j/c_i}{x_i-x_j}, \text{ and}$$

$$(\mathbf{D}_N)_{jj} = (2/l) \phi'_j(x_j) = -\sum_{i \neq j} (\mathbf{D}_N)_{ij}$$

are entries into the spectral differentiation matrix  $\mathbf{D}_N$ . The factor  $(2/l)$  is due to the projection from the physical domain  $[0, l]$  to the interval  $[-1, 1]$ , discussed before.

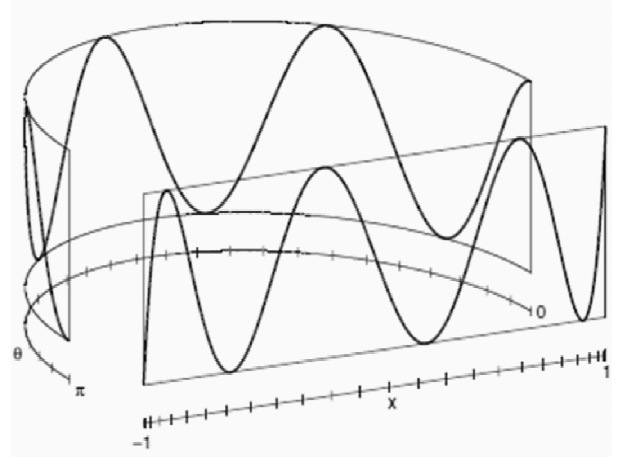


**Figure 1:** Projection of cosine in function of  $\theta$  (equispaced points) to Chebyshev polynomial in function of  $x$  (points clustered towards the ends of the interval).

## 2.3 Space Discretization

Finally, we use approximations of the spatial derivatives (6) in the matrix form,

$$y'_k(\mathbf{x},t) = \mathbf{D}_N y_k(\mathbf{x},t), \quad k=1,2,\dots,N_y, \quad (7)$$

where

$$y_k(\mathbf{x},t) = [y_k(x_0,t) \quad y_k(x_1,t) \quad \dots \quad y_k(x_N,t)]^T,$$

to convert (1) into a system of  $N_y(N+1)$  linear differential equations:

$$(\mathbf{A} \otimes \mathbf{I}_{N+1}) \frac{d}{dt} \mathbf{y}_N(t) = (\mathbf{B} \otimes \mathbf{I}_{N+1}) \mathbf{y}_N(t) + (\mathbf{I}_{N_y} \otimes \mathbf{D}_N) \mathbf{y}_N(t), \quad (8)$$

where

$$\mathbf{y}_N(t) = [y_1(\mathbf{x},t)^T \quad \dots \quad y_k(\mathbf{x},t)^T \quad \dots \quad y_{N_y}(\mathbf{x},t)^T]^T,$$

$\otimes$  is the Kronecker product, and  $\mathbf{I}_{N+1}$  and  $\mathbf{I}_{N_y}$  are identity matrices with sizes  $(N+1) \times (N+1)$  and  $N_y \times N_y$  respectively. The model (8) can be written in the form

$$\frac{d}{dt} \mathbf{y}_N(t) = \mathbf{F} \mathbf{y}_N(t), \quad (9)$$

where

$$\mathbf{F} = (\mathbf{A} \otimes \mathbf{I}_{N+1})^{-1} [(\mathbf{B} \otimes \mathbf{I}_{N+1}) + (\mathbf{I}_{N_y} \otimes \mathbf{D}_N)],$$

$$\mathbf{F} \in \mathbf{R}^{N_y(N+1) \times N_y(N+1)},$$

and it can be solved using a standard ODE solver for specified initial and boundary conditions.

### 3 APPLICATION EXAMPLE AND DISCUSSION

#### 3.1 The transmission line example

Three-phase 50Hz, 300km long unsymmetrical transmission line, with the towers constructed according to Fig. 2, and parameters in Table 1, has been selected to demonstrate application of the Chebyshev pseudo-spectral discretization in simulation of electromagnetic transients.

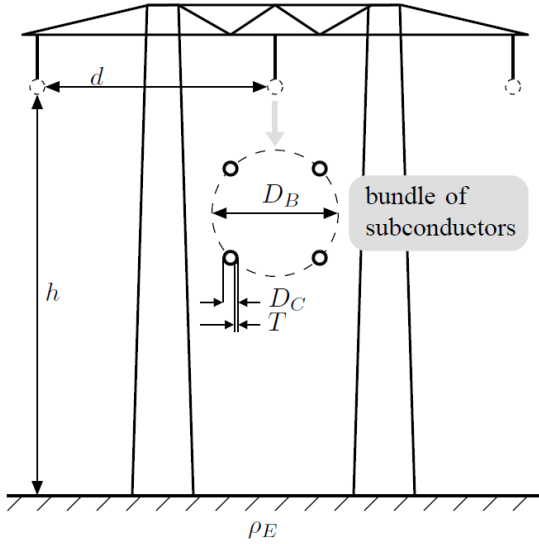


**Figure 2:** Three-phase transmission line tower (parameters in Table 1)

Quantity	Symbol	Value
height [m]	$h$	20.7
bundle distance [m]	$d$	12.8
bundle diameter [cm]	$D_B$	64.66
conductor diameter [cm]	$D_C$	3.56
ratio of hollow cylinder	$T/D_C$	0.375
conductor DC resist. [ $\Omega/km$ ]	$R_C$	0.043
ground resistivity [ $\Omega m$ ]	$\rho_E$	100

**Table 1:** Three-phase transmission line parameters

Assuming that the tower geometry in Fig.2 and corresponding parameters in Table 1 are not changing along the full line length, we calculated the electrical

parameters of the line using the SIMULINK SimPower-Systems™ function *Compute RLC Line Parameters* [10]. The matrix  $\mathbf{G}$  is a zero matrix and the computed RLC parameters are:

$$\mathbf{R} = \begin{bmatrix} 58.221 & 47.104 & 47.063 \\ 47.104 & 58.224 & 47.104 \\ 47.063 & 47.104 & 58.221 \end{bmatrix} \quad m\Omega / km,$$

$$\mathbf{L} = \begin{bmatrix} 1.6876 & 0.8652 & 0.7267 \\ 0.8652 & 1.6876 & 0.8652 \\ 0.7267 & 0.8652 & 1.6876 \end{bmatrix} \quad mH / km, \text{ and}$$

$$\mathbf{C} = \begin{bmatrix} 11.305 & -2.446 & -0.8203 \\ -2.446 & 11.775 & -2.446 \\ -0.8203 & -2.446 & 11.305 \end{bmatrix} \quad nF / km.$$

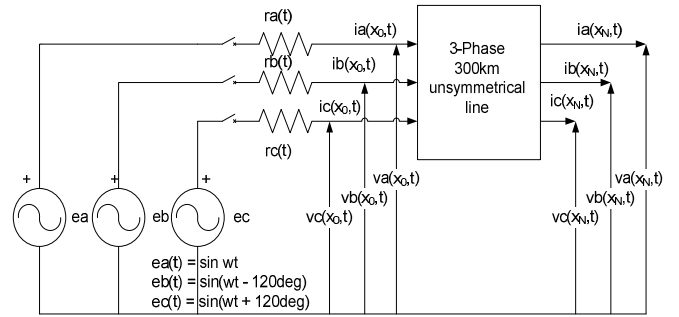


**Figure 3:** Circuit diagram of the simulation example [6]

To demonstrate the performance of the proposed method, we are using the example shown in Fig. 3 which was studied before by Talukdar [6]. Boundary conditions in this example are derived using circuits connected to the sending and receiving ends of the line. The receiving-end of the line is open and the corresponding boundary conditions are defined using three injection currents, in each phase, equal to zero:

$$ia(x_N, t) = ib(x_N, t) = ic(x_N, t) = 0, \quad (10)$$

where  $x_N = 1$  is the last Chebyshev point in the computational domain  $[-1,1]$  corresponding to the receiving-end of the line.

The sending line end is connected to the system represented with a Thevenin's equivalent. The voltage source of this equivalent ( $ea(t), eb(t), ec(t)$ ) is three-phase sinusoidal, single-frequency (50Hz), balanced source with the amplitude in each phase equal to 1pu. Impedance of the equivalent is resistive and it is changing in time to simulate events in the system which will initiate transients on the line. The boundary conditions at the sending-end (i.e. at  $x_0 = -1$ ; the first Chebyshev point in the computational domain  $[-1,1]$ ) are [6]:

a-phase boundary condition:

$$va(x_0, t) = ea(t) - r_a(t) \times ia(x_0, t), \quad r_a(t) \neq \infty, \quad (11)$$

b-phase boundary condition:

$$\begin{cases} \text{ib}(x_0,t) = 0, & \text{if } r_b(t) = \infty, \\ \text{vb}(x_0,t) = \text{eb}(t) - r_b(t) \times \text{ib}(x_0,t), & \text{if } r_b(t) \neq \infty, \end{cases} \quad (12)$$

and

c-phase boundary condition

$$\begin{cases} \text{ic}(x_0,t) = 0, & \text{if } r_c(t) = \infty, \\ \text{vc}(x_0,t) = \text{ec}(t) - r_c(t) \times \text{ic}(x_0,t), & \text{if } r_c(t) \neq \infty, \end{cases} \quad (13)$$

where

$$\begin{aligned} & (\text{va}(x_0,t), \text{vb}(x_0,t), \text{vc}(x_0,t)) \text{ and} \\ & (\text{ia}(x_0,t), \text{ib}(x_0,t), \text{ic}(x_0,t)) \end{aligned}$$

are three-phase voltages and currents respectively at the sending-end; and the time-varying resistances are [6]:

$$r_a(t) = \begin{cases} 415\Omega, & \text{if } 0 \leq t < 10\text{ms}, \\ 15\Omega, & \text{if } t \geq 10\text{ms}, \end{cases} \quad (14)$$

$$r_b(t) = r_c(t) = \begin{cases} \infty, & \text{if } 0 \leq t < 4\text{ms}, \\ 415\Omega, & \text{if } 4\text{ms} \leq t < 14\text{ms}, \\ 15\Omega, & \text{if } t \geq 14\text{ms}. \end{cases} \quad (15)$$

### 3.2 The line model with included boundary conditions

Certain differential equations in the system (9) related to the boundary conditions, as defined in the example in Section 3.1, should be removed. Which equations are removed depends on the switching events:

- 0ms – phase *a* connected to the voltage source,
- 4ms – phases *b* and *c* connected to the voltage source,
- 10ms – phase *a* source resistance reduced to 15Ω, and
- 14ms – phases *b* and *c* resistances reduced to 15Ω.

The boundary *abc* voltages, according to the equations (11) - (13), are functions of currents and source voltages as well as switching events (e.g. time-varying resistances). There are 6 boundary conditions which are changing in time. The following variables represent boundary conditions:

- $0 \leq t < 4\text{ms} \rightarrow$  the sending-end voltage in phase *a* and five currents (phases *b* & *c* at sending-end and all receiving-end currents);
- $t \geq 4\text{ms} \rightarrow$  three voltages at sending-end and three currents at receiving-end.

To remove differential equations representing boundary conditions we remove 6 rows in the matrix **F** of the system (9) having indices in the time-varying vector **b**:

$$- 0 \leq t < 4\text{ms} \rightarrow \mathbf{b} = [ \underbrace{1 \quad 4N+5 \quad 5N+6}_{\text{sending-end}} \quad \underbrace{4(N+1) \quad 5(N+1) \quad 6(N+1)}_{\text{receiving-end}} ],$$

$\text{va}(x_0,t), \text{ib}(x_0,t), \text{ic}(x_0,t)$        $\text{ia}(x_N,t), \text{ib}(x_N,t), \text{ic}(x_N,t)$

$$- t \geq 4\text{ms} \rightarrow \mathbf{b} = [ \underbrace{1 \quad N+2 \quad 2N+3}_{\text{sending-end}} \quad \underbrace{4N+4 \quad 5N+5 \quad 6N+6}_{\text{receiving-end}} ].$$

$\text{va}(x_0,t), \text{vb}(x_0,t), \text{vc}(x_0,t)$        $\text{ia}(x_N,t), \text{ib}(x_N,t), \text{ic}(x_N,t)$

The resulting matrix is split in two parts:

**F<sub>a</sub>** (squared matrix); contains all columns except those with indices in **b**, and

**F<sub>b</sub>**; contains remaining columns having indices in **b**.

The resulting system of  $6N$  differential equations is:

$$\frac{d}{dt} \bar{\mathbf{y}}_N(t) = \mathbf{F}_a \bar{\mathbf{y}}_N(t) + \mathbf{F}_b f(\bar{\mathbf{y}}_N(t), \mathbf{u}(t), t), \quad (16)$$

where

$\bar{\mathbf{y}}_N(t)$  are all non-boundary variables in the vector  $\mathbf{y}_N(t)$ , and

$f(\bar{\mathbf{y}}_N(t), \mathbf{u}(t), t)$  are boundary functions (e.g. (11)-(13)) representing boundary circuits.

In the functions  $f(\bar{\mathbf{y}}_N(t), \mathbf{u}(t), t)$  inputs  $\mathbf{u}(t)$  are voltage sources ( $\text{ea}(t), \text{eb}(t), \text{ec}(t)$ ). Since the boundary functions in our example are linear and time-varying, it is possible to split  $f(\bar{\mathbf{y}}_N(t), \mathbf{u}(t), t)$  in the part which is in function of  $\bar{\mathbf{y}}_N(t)$  and the part in function of  $\mathbf{u}(t)$ . Using this form of  $f(\bar{\mathbf{y}}_N(t), \mathbf{u}(t), t)$  we can rewrite (16) as the time-varying system of linear differential equations:

$$\frac{d}{dt} \bar{\mathbf{y}}_N(t) = \mathbf{H}_a(t) \bar{\mathbf{y}}_N(t) + \mathbf{H}_b(t) \mathbf{u}(t), \quad (17)$$

where the matrices  $\mathbf{H}_a(t)$  and  $\mathbf{H}_b(t)$  are changing in time due to switching events.

The system of ODEs (17) is solved using Adams-Bashforth-Moulton PECE solver [11] implemented in MATLAB as ode113 function [10] with the tolerances  $\text{RelTol}=\text{AbsTol}=1\text{e-}6$ . The initial conditions for this example are:  $\bar{\mathbf{y}}_N(0) = 0$ .

### 3.3 Results and discussion

First 20ms of three-phase voltage and current waveforms at sending-end of the transmissions line after switching-in phase *a* are shown in Figures 4 and 5. During this period 4 switching events, including switching-in phase *a*, occurred which gave rise to transients in time and spatial wave propagation. These simulated waveforms are obtained by solving the system of differential equations (17) obtained through spatial discretization having  $N+1=201$  Chebyshev points. The total number of equations in this system after including the boundary conditions (specified in sections 3.1 and 3.2) is  $6N=1200$ . Figure 6 shows phase *b* voltage wave propagation after switching events at 4ms, 10ms and 14ms.

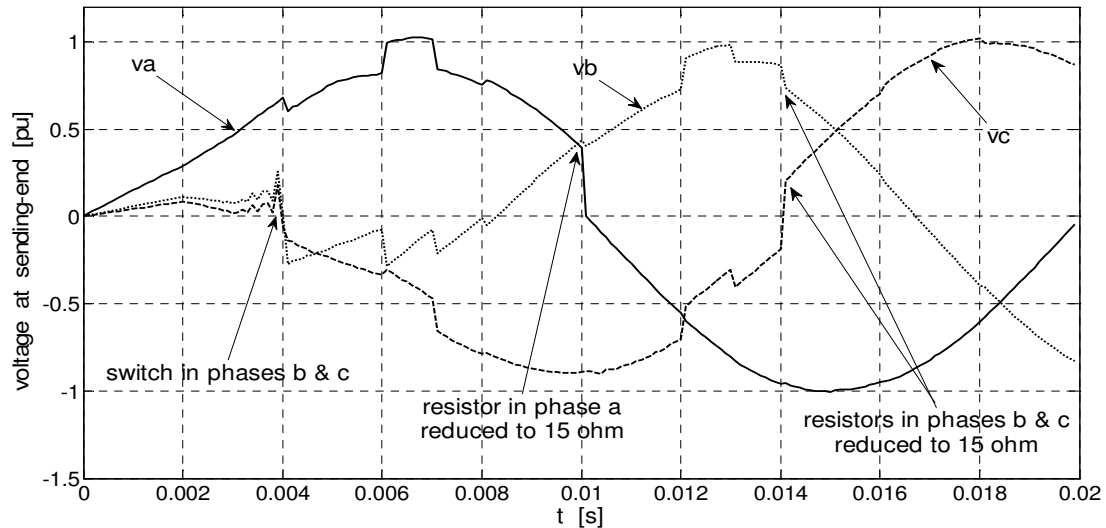


**Figure 4:** Three-phase sending-end voltages during switching events simulated with spectral discretization having  $N+1 = 201$  points

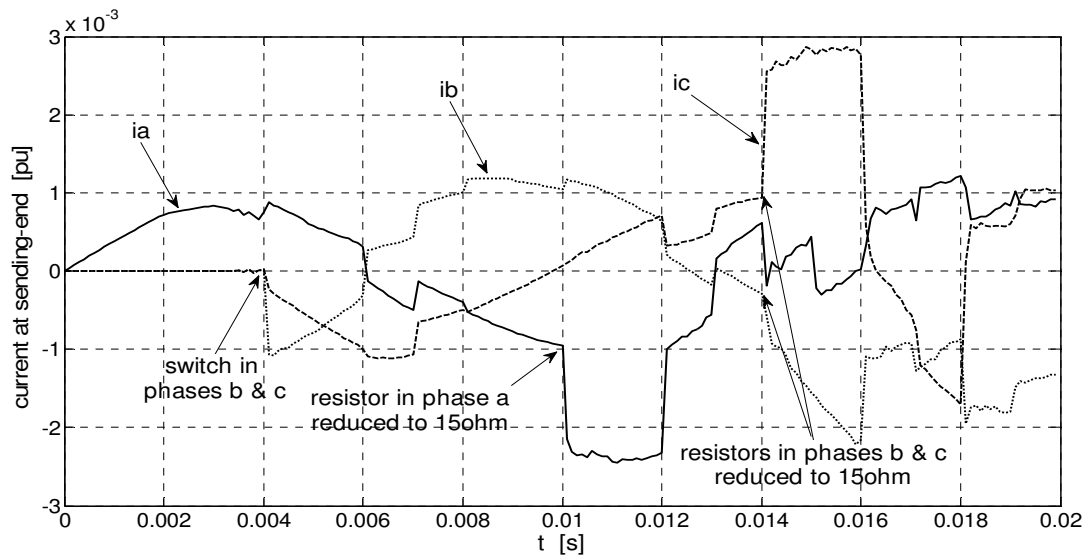


**Figure 5:** Three-phase sending-end currents during switching events simulated with spectral discretization having  $N+1 = 201$  points

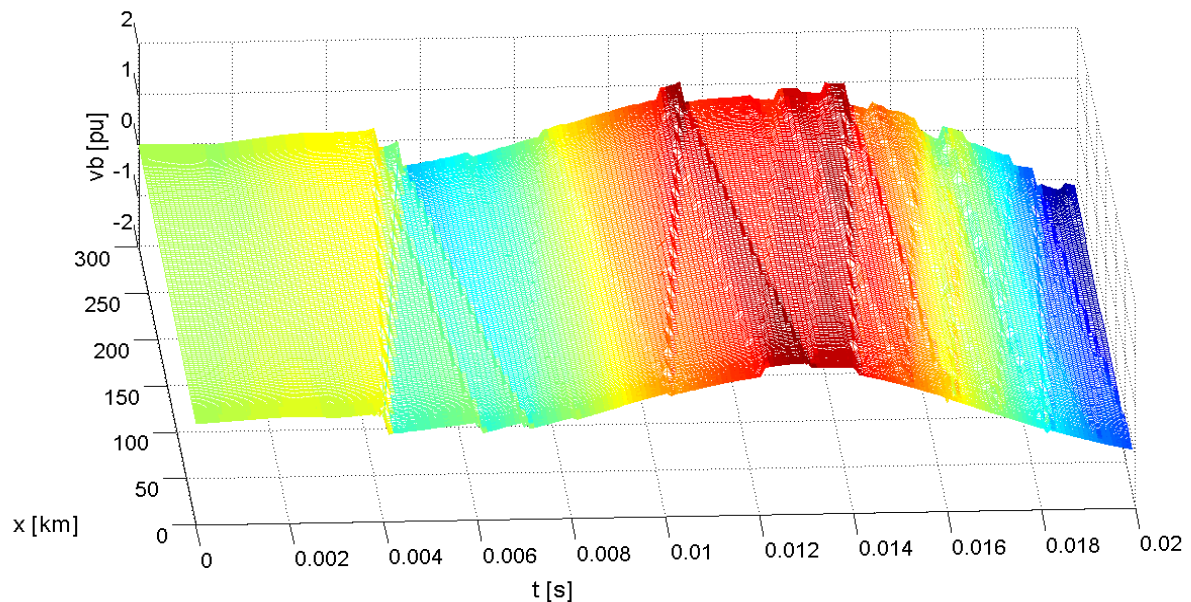


**Figure 6:** Voltage wave propagation in phase *b* during switching events simulated with spectral discretization ( $N+1 = 201$  points)

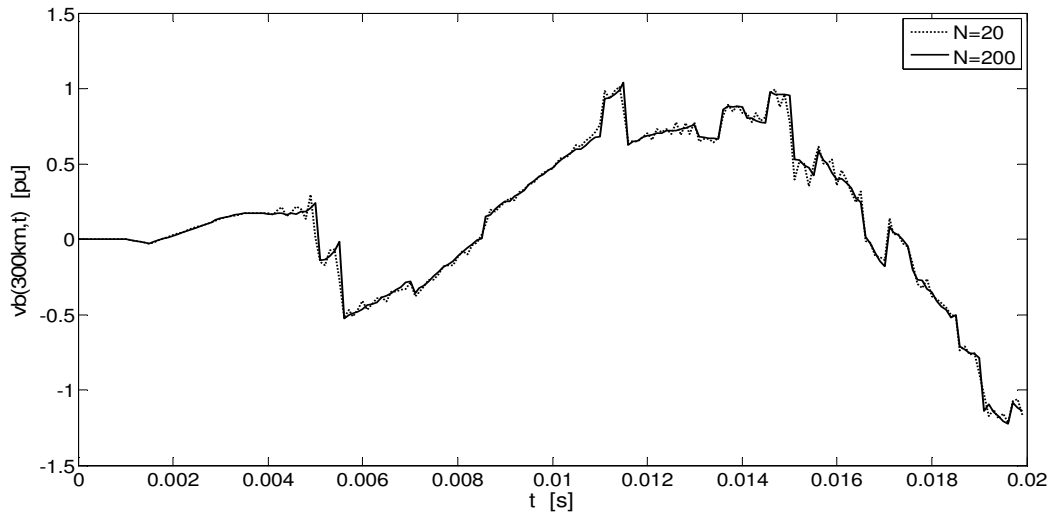


**Figure 7:** Comparison of receiving-end voltage waveforms in phase  $b$ , simulated during switching events using coarse ( $N = 20$ ) and refined ( $N = 200$ ) spectral discretizations

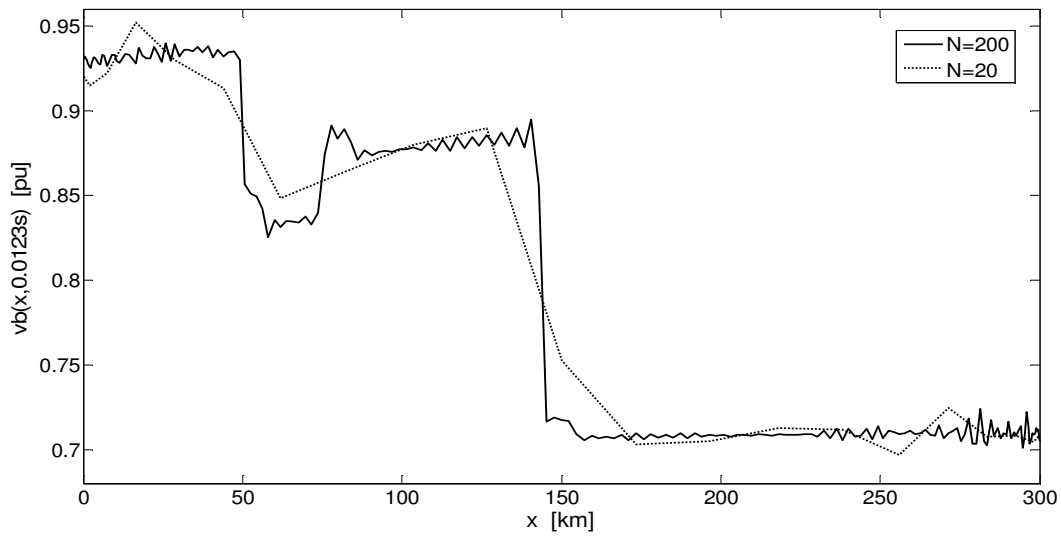


**Figure 8:** Comparison of spatial variations of the voltage in phase  $b$  at time  $t = 0.0123s$ , simulated using coarse ( $N = 20$ ) and refined ( $N = 200$ ) spectral discretizations

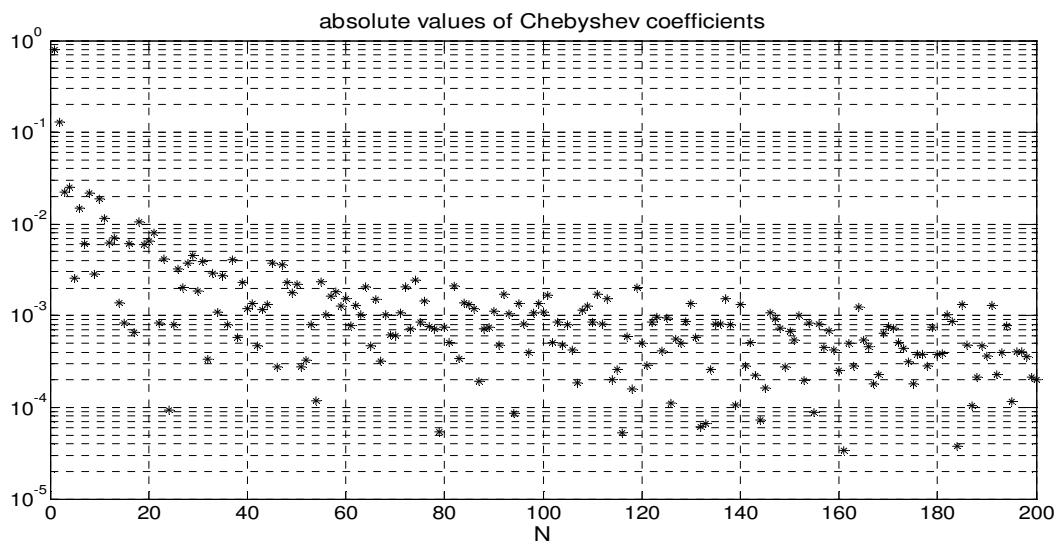


**Figure 9:** Coefficients ( $a_j(t)$ ,  $j=0,1,\dots,N$ ,  $N=200$ ) of the Chebyshev expansion (5) modeling spatial variation of the voltage in phase  $b$  at time  $t = 0.0123s$  (see Fig. 8)

In order to illustrate the effect of spatial grid density on the transmission line simulation result, the solution of the PDEs (1) with coarse spectral discretization ( $N = 20$ ) has been performed. In this computation, the number of ODEs in the system (17) is reduced to  $6N = 120$ . As can be seen in Figures 7 and 8, with the lower number of spatial discretization points, additional oscillations due to numerical errors are present in time and some details in spatial waveforms are lost.

The spatial accuracy at time  $t$  can be checked by recognizing that the sub-vectors of the solution vector  $\mathbf{y}_N(t)$ , representing spatial waveforms of each voltage or current (in total 6 sub-vectors), are interpolants defined on  $N+1$  Chebyshev points. These interpolants can be converted into the Chebyshev expansion (5) using the DCT transformation. Fig. 9 shows coefficients of the Chebyshev expansion of the voltage spatial variation in Fig. 8. Slow decrease in the coefficient values as the index increases points to slow convergence of the Chebyshev expansion. Further refinement of the Chebyshev grid would bring only minor improvement in accuracy. The reason for slow convergence is a number of abrupt changes in the spatial voltage variation (see Fig. 8) which are associated with the travelling waves. The Chebyshev points are distributed denser on the edges of the interval  $[0, 300\text{km}]$  than in the middle, and therefore there is always proportionally smaller number of points to represent the abrupt changes in the middle.

#### 4 CONCLUSIONS

A computational method based on the Chebyshev pseudo-spectral discretization is proposed to solve the system of PDEs with constant coefficients that are modeling unsymmetrical transmission lines. The discretization procedure converts the distributed-parameter PDE model with specified boundary conditions into a system of ODEs. The method approximates spatial-variations of the variables by finite Lagrange polynomial interpolation at Chebyshev points. The interpolants are constructed using numerically stable and computationally effective barycentric interpolation formula. Approximation of spatial derivative is directly available through interpolant derivative. Solution accuracy for specific spatial grid resolution is estimated by converting spatial Chebyshev interpolants into the Chebyshev polynomial expansion (using the DCT algorithm) and evaluating values of the expansion coefficients. To demonstrate the numerical behavior and accuracy of the proposed method, the results of simulation of the unsymmetrical line during switching events are presented. Combined with the ODE solver, the Chebyshev pseudo-spectral discretization method achieves acceptable level of accuracy with the modest number of grid points. The method proposed in this paper can be used in simulation of switching transients on the unsymmetrical transmission lines as well as for line parameter identification using synchronized event records.

#### ACKNOWLEDGMENT

The authors would like to thank the *Deutsche Forschungsgemeinschaft (German Research Foundation)* for supporting this research.

#### REFERENCES

- [1] R. Schulze and P. Schegner, "Parameter identification of unsymmetrical transmission lines," *IEEE PES PowerTech*. Bucharest, Romania, 28 June - 2 July 2009.
- [2] R. Zivanovic, P. Schegner, O. Seifert, and G. Pilz, "Identification of the resonant-grounded system parameters by evaluating fault measurement records," *IEEE Transactions on Power Delivery*, Vol. 19, No. 3, pp. 1085–1090, July 2004.
- [3] R. Schulze, P. Schegner, and R. Zivanovic, "Parameter Identification of Unsymmetrical Transmission Lines Using Fault Records Obtained from Protective Relays", *IEEE Transactions on Power Delivery*, Vol. 26, No. 2, pp. 1265- 1272, April 2011
- [4] B. Fornberg, *A Practical Guide to Pseudo-spectral Methods*. Cambridge University Press, New York, 1996
- [5] L. Hofmann, *Modellierung von Freileitungen mit frequenzabhängigen Parametern im Kurzzeitbereich*, Ph.D. dissertation, Universität Hannover, 1997
- [6] S. Talukdar, " Algorithms for the simulation of transients in multiphase variable parameter transmission lines", *IEEE Winter Power Meeting*, 1971
- [7] F. M. Tesche, M. V. Ianoz, and T. Karlsson, *EMC Analysis Methods and Computational Models*. John Wiley & Sons, Inc., 1997.
- [8] H.E. Salzer, "Lagrangian interpolation at the Chebyshev points  $x_{n,v} = \cos(v\pi/n)$ ,  $v=0(1)n$ ; some unnoted advantages", *The Computer Journal*, Vol. 15, No. 2, 1972, pp. 156-159
- [9] V.E. Neagoie, "Chebyshev Nonuniform Sampling Cascaded with the Discrete Cosine Transform for Optimum Interpolation, *IEEE Transactions Acoustics Speech and Signal Processing*. Vol. 38. No. 10. October 1990
- [10] [www.mathworks.com](http://www.mathworks.com)
- [11] Shampine, L. F. and M. K. Gordon, *Computer Solution of Ordinary Differential Equations: the Initial Value Problem*, W. H. Freeman, San Francisco, 1975.